Characterization of Au catalysts

by T. van Heerden*, M. Hill*, J. Case*, and E. van Steen*

Synopsis

A range of supported gold catalysts was prepared by ion exchange, varying many of the preparation variables, including concentration in the precursor solution, washing procedure, as well as drying and calcination procedures. These catalysts have been characterized extensively. TEM images show essentially the same crystallite size distributions, between 2–5 nm, for almost all catalysts, the only exception being catalysts not washed in ammonia, which did not show any small crystallites. Additional characterization with SEM yielded an interesting discovery. Catalysts that appear identical on the TEM also contain some large crystallites in the range of 50–500 nm. Differences in dispersion due to the drying procedure not seen on the TEM can now be observed. Oxygen chemisorption is being investigated as an additional method to characterize gold based catalysts to complement the typically used electron microscope techniques.

Keywords
Gold catalyst, TEM, SEM, characterization, ion exchange, particle size.

Introduction

It has been shown that supported gold particles of sizes in the nanometer range are active catalysts for CO oxidation, one of the most studied reactions on this catalyst. In contrast, the hydrogenation of CO has not been investigated much, with slightly more of the literature dealing with CO_2 hydrogenation. Gold particles below 5 nm are reported to catalyse the production of methanol by hydrogenation of CO[1]. Formation of alcohols, primarily methanol, by hydrogenation of CO and CO_2 has been demonstrated over a range of supported gold catalysts[2–4].

Methanol is a chemical used in large quantities primarily for the production of formaldehyde and the fuel additive methyl tert-butyl ether (MTBE). The traditional route for the synthesis of methanol occurs at temperatures of approximately 240–260°C and pressures of 50–80 bar over catalysts containing CuO and ZnO. A more active catalyst would allow a reduction in the reaction pressure by operating at a lower temperature, resulting in significantly lower operating costs.

A variety of preparation methods are known for the synthesis of nano-sized gold on support materials[5–8]. Ion exchange has been well studied in the preparation of other metal catalysts, but is less commonly used in gold catalyst preparation[9], possibly due to the presence of chloride ions in anionic exchange with $HAuCl_4^-$, and the limited number of available cationic gold complexes.

Previous studies have shown the resulting gold crystallite size to have a significant effect on the activity (per unit mass of catalyst) of gold catalysts. These catalysts are most commonly characterized for particle size by transmission electron microscopy (TEM) and X-ray diffraction (XRD). Both of these methods become somewhat subjective at low loadings and for catalysts with small gold crystallites.

Due to the presence of primarily small crystallites, TEM is the preferred method for characterization of gold catalysts. SEM is not often used and thus the presence of larger gold crystallites may have gone unnoticed for many supported gold catalysts.

Experimental

Catalyst preparation

Anionic ion exchange was used to prepare well-dispersed gold catalysts supported on γ-Al_2O_3 (Puralox SCCa 5-150, Sasol Germany; S_{BET} = 162 m²/g, Vpore = 0.47 cm³/g, d_p < 500 µm). This method requires a pH in the supernatant solution below the iso-electric point (IEP) of the support, which was estimated to be approximately 8.2. The catalysts were typically prepared by contacting a solution containing 0.5 g Au (prepared from a stock solution containing 250 g Au per litre supplied by Mintek), the pH of which was adjusted to approximately 5 (unless otherwise

* *Centre for Catalysis Research, Department of Chemical Engineering, University of Cape Town.*

Characterization of Au catalysts

Table I

Variables studied in the catalyst preparation

	Precursor		Aging			Washing	Ammonia wash			2nd water wash	drying			Calcination		
catalyst code	Au conc. (g/L)	pH	pH (initial)	support concentration (g/L)	pH (final)	1st water wash water volume (ml/gcat)	duration (min)	ammonia concentration (g/g)	catalyst/ammonia ratio (g/L)	water volume (ml/gcat)	duration (hours)	temperature (°C)	environment	duration (hrs)	temperature (°C)	environment
A1-200	1	4.90	5.25	20	5.03	50	20	25%	20	50	overnight	60	air	16	200	hydrogen
A1-500	1	4.90	5.25	20	5.03	50	20	25%	20	50	overnight	60	air	16	500	hydrogen
A2-200H	25	5.20		500		50	20	25%	20	50	overnight	60	air	16	200	hydrogen
A2-200Ar	25	5.20		500		50	20	25%	20	50	overnight	60	air	16	200	argon
A2-500H	25	5.20		500		50	20	25%	20	50	overnight	60	air	16	500	hydrogen
A2-500Ar	25	5.20		500		50	20	25%	20	50	overnight	60	air	16	500	argon
B-base	1	4.96	5.38	20	5.08	50	20	25%	20	50	overnight	60	air	4	200	hydrogen
B-time	1	4.96	5.38	20	5.08	50	5	25%	20	50	overnight	60	air	4	200	hydrogen
B-conc	1	4.96	5.38	20	5.08	50	20	0.2%	20	50	overnight	60	air	4	200	hydrogen
B-ratio	1	4.96	5.38	20	5.08	50	20	25%	2	50	overnight	60	air	4	200	hydrogen
B-none	25	4.78		500	5.87	50	0	-	-	-	overnight	60	air	18.5	200	air
C-DRY	0.5	4.98	4.63	10	4.80	100	20	25%	20	50	2	200	flowing dry air	2	200	hydrogen
C-WET	0.5	4.98	4.63	10	4.80	100	20	25%	20	50	2	200	flowing wet air	2	200	wet hydrogen
C60	0.5	5.02	4.85	10	5.01	100	20	25%	20	50	-	60	rotavap 110mbar	2	200	hydrogen
C80	0.5	5.02	4.85	10	5.01	100	20	25%	20	50	-	80	rotavap 110mbar	2	200	hydrogen
C100	0.5	5.02	4.85	10	5.01	100	20	25%	20	50	-	100	rotavap 110mbar	2	200	hydrogen
D100	0.5	3.11	3.27	10	3.99	100	20	25%	20	50	2	200	air	18	100	hydrogen
D200	0.5	3.08	3.21	10	3.96	100	20	25%	20	50	2	200	air	18	200	hydrogen
D300	0.5	3.06	3.14	10	3.74	100	20	25%	20	50	2	200	air	18	300	hydrogen
D400	0.5	3.10	3.24	10	4.27	100	20	25%	20	50	2	200	air	18	400	hydrogen
D500	0.5	3.27	3.37	10	3.96	100	20	25%	20	50	2	200	air	18	500	hydrogen

stated) using a dilute NaOH solution, with 10 g of the support. The suspension was aged for 22 hours at room temperature under stirring. The catalyst precursor was subsequently filtered off and washed with 1 ℓ deionized water. The catalyst precursor was then redispersed in 500 ml of an aqueous 25 wt.% NH_3 solution to remove the chloride ions[10,11], which are thought to cause sintering and/or blockage of the catalytically active sites[12,13]. The catalyst precursor was subsequently filtered off after 20 minutes and washed with 500 ml deionized water. The supported material was dried and subsequently calcined in a fluidized bed reactor.

An overview of the preparation variables for each of the synthesized catalysts is given in Table I.

The influence of the concentration of the gold in the initial supernatant solution was investigated in Batch A. Initial gold concentrations were varied between 1 and 50 g Au per litre at an initial pH of approximately 5.0. Catalysts were dried in an oven operating at 60°C for 16 hours after washing, before being calcined for 16–18 hours in hydrogen or argon (50 ml(NTP) /min) at temperatures ranging from 200–500°C.

The influence of the ammonia washing step was investigated in Batch B, which was prepared by contacting the support with a supernatant solution containing initially 1 g Au per litre at an initial pH of approximately 5.0. The concentration of the ammonia solution was varied between 0 and 25 wt.%, and the duration of the ammonia wash was varied between 0 and 20 minutes.

The effect of the drying conditions was investigated with Batch C, which was prepared using a supernatant solution containing 0.5 g Au per litre at a pH of approximately 5.0. The catalyst precursor was dried either in the fluidized bed reactor or under reduced pressure in a rotary evaporator. Dry air (50 ml(NTP)/min) or air (50 ml(NTP)/min) saturated with water at room temperature (y_{H_2O} = 0.03) was used for the drying process in the fluidized bed reactor at 200°C for 2 hours. Drying in the rotary evaporator was performed at 110 mbar and 60, 80, and 100°C, respectively. Subsequently, the catalyst was either calcined in dry hydrogen (50 ml(NTP)/min) or in hydrogen (50 ml(NTP)/min) saturated with water at room temperature (y_{H_2O} = 0.03) at 200°C for 2 hours.

The influence of the calcination temperature was investigated for Batch D, which was prepared using a supernatant solution containing 0.5 g Au per litre at a pH of approximately 3.2. The catalysts were dried in an oven at 200°C for 2 hours. Each of the catalysts was calcined in hydrogen (50 ml(NTP)/min) for 2 hours at 100, 200, 300, 400, and 500°C, respectively.

Catalyst characterization

Gold loading on each catalyst was determined using atomic absorption spectroscopy (AAS) following digestion of samples of the catalyst in HCl/HF. The gold crystallite size distribution on the synthesized catalysts was estimated from TEM images recorded on a JEM 1200EXII (JEOL) operating at 120 kV. Some catalysts were evaluated using HR-TEM (FEI/Tecnai F20 Cryo TWIN FEGTEM) operating at 200 kV. The large gold crystallites present in the samples were recorded using SEM (Nova NanoSEM 230) operating at either 15 or 20 keV.

Some of the catalysts were further characterized by oxygen chemisorption, similar to the method used by Berndt *et al.*[14]. Oxygen chemisorption measurements were conducted using a Micrometrics ASAP 2020C. The catalyst was heated in hydrogen to 200°C, and kept at this temperature for 16 hours. The sample was subsequently evacuated for 2 hours. The oxygen uptake was measured at 200°C with pressures between 0.1mm Hg and 700 mm Hg.

Results and discussion

Catalyst loading

The gold loading and uptake of each catalyst is shown in Table II. Uptakes from 37 percent to 53 percent are obtained. Preliminary work has shown that an uptake of between 30 and 50 percent is typical for this system (Au/Al_2O_3 prepared by ion exchange with a $HAuCl_4$ precursor), and that a maximum uptake is usually obtained when the catalyst is prepared at a pH of approximately 5. This maximum uptake has also been demonstrated for Au/Al_2O_3 catalysts prepared by deposition precipitation[13].

Crystallite size distribution

All the average crystallite sizes obtained using TEM (as well as SEM) are given in Table III. All catalysts (with the exception of B-none) were found to predominantly contain gold crystallites between 2 and 5 nm when examined with TEM.

As an example, crystallite size distributions determined using TEM, as well as some TEM images from batch D, are shown in Figure 1. Although the calcination temperature was varied from 100–500°C to encourage the sintering of the gold crystallites, the average sizes decreased slightly over the 200–400°C range before increasing fractionally at 500°C.

It is important at this point to note that these histograms describe only the crystallites in the size range that is visible using TEM. The limitations are somewhat dependent on the apparatus and the support material used. In our case, crystallites with a size of less than 2 nm are not easily seen on the TEM images. Crystallites larger than 20 nm were very rarely encountered on the TEM.

For this reason, to check if the crystallites below 2 nm played a significant role in the particle size distribution, HRTEM was conducted on catalysts D200, D300, and D400. It was found that particle size distributions obtained from HRTEM mimic those of the TEM; however, the increased visibility of particles less than 2 nm in size results in a slightly smaller average particle size.

Table II

Catalyst loading and gold uptake

Batch/ Catalyst	Loading (wt%)	pH of preparation	Gold uptake
Batch A	2.3 ± 0.09	5	46%
Batch B*	1.8 ± 0.2	5	37%
Batch C	2.7 ± 0.03	5	53%
Batch D	2.2 ± 0.2	3	43%

*catalysts B-none, B-base, and B-time are not included in this table, their analysis is still outstanding

Characterization of Au catalysts

For batches A and C, where calcination conditions, drying conditions, and precursor concentrations were varied, the distributions obtained for all catalysts are similar to those in batch D300–500. There is no significant difference between the distributions of the various batches.

With batch B, the size distributions are similar to those of catalysts D100 and D200 with a slightly larger average. However, for the catalyst that was not washed in ammonia (B-none) hardly any gold crystallites were visible on the TEM images. Those crystallites that were found were of a much larger size than encountered in the other samples (>50 nm).

It is interesting to compare these results with those obtained using SEM. Catalysts previously believed to have crystallite size distributions of 2–5 nm based on TEM analysis, have been shown to contain various amounts of large (>50 nm) gold crystallites. This is illustrated with the catalysts of batch D shown in Figure 2.

Most of the supported gold catalysts investigated under SEM displayed at least a few large particles (>50 nm) regardless of the preparation conditions used. However, while some catalysts displayed very few large gold particles, others were essentially covered in them. There was also a visible difference in the degree of homogeneity displayed by certain catalysts. While it is almost impossible to quantify these two phenomena in a meaningful way (nonetheless average particle sizes obtained from SEM images are given in Table III), a qualitative look at the SEM images yields some interesting observations.

For batches A, C, and D, there is no significant difference in the large particles found on the SEM images within that batch. And while the error on the average crystallite sizes obtained from the images is high, it is unlikely that the calcination conditions or the initial precursor solution concentrations play a significant role in the formation of these larger gold particles. In batch B, however, there is a clear effect of the washing procedure on the formation of

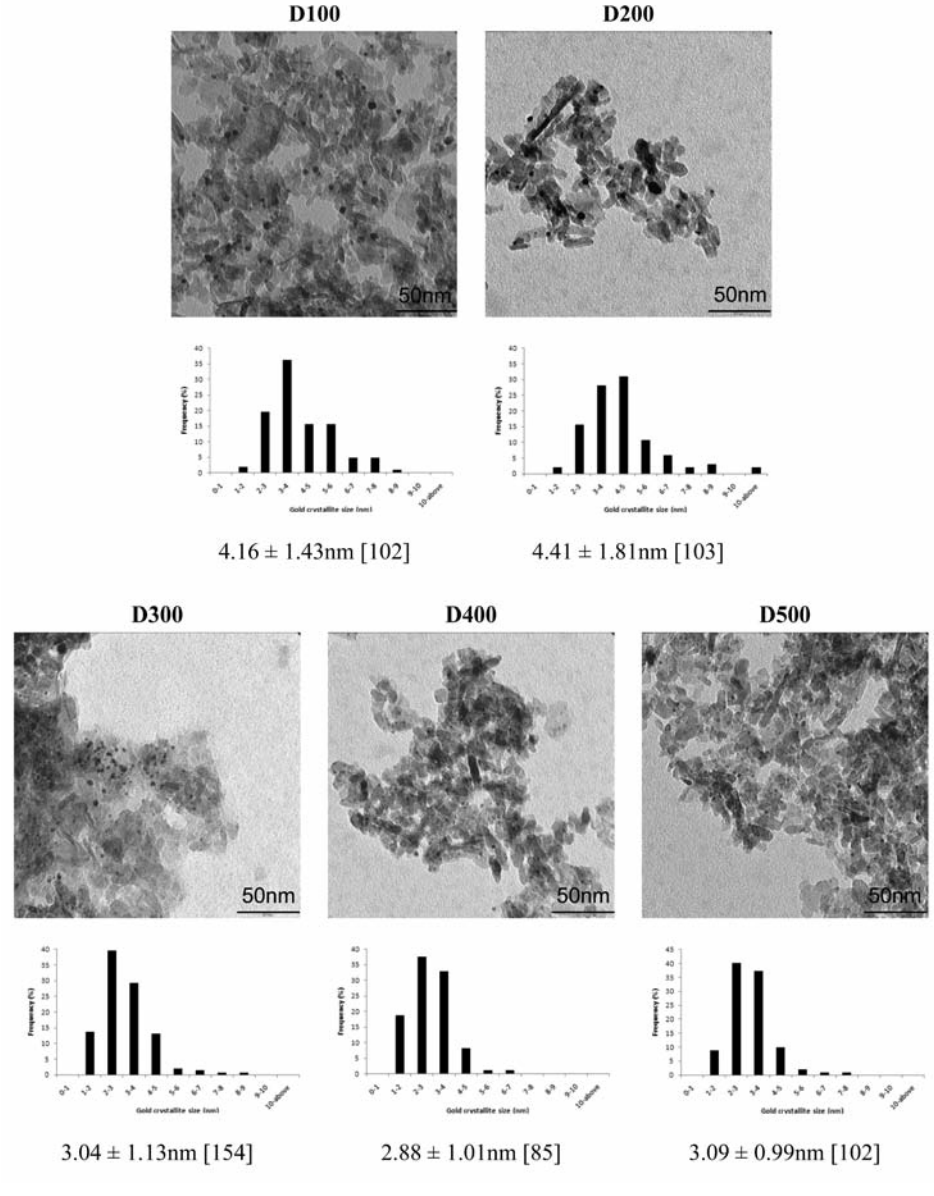

Figure 1—Examples of TEM images and the resulting crystallite size distributions [no. of particles measured in brackets]- Batch D

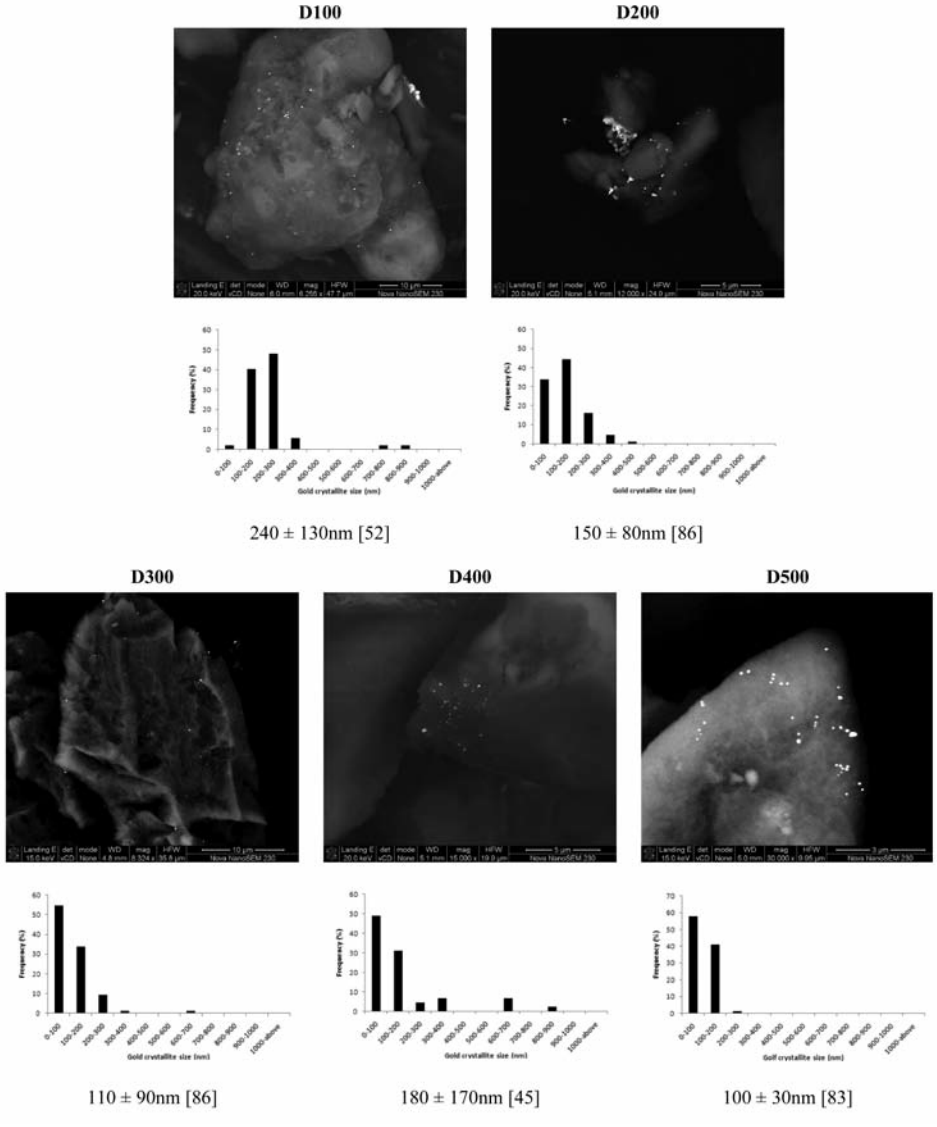

Figure 2—Examples of SEM images and resulting crystallite size distributions [no. of particles measured in brackets] - Batch D

larger gold particles. The catalyst prepared without any ammonia wash (catalyst B-none) contains a significantly higher amount of large gold crystallites compared with any other catalyst investigated. As discussed previously, almost no gold crystallites were found, this catalyst under the TEM and those that were observed were of the larger variety. However, the remaining catalysts in this batch were similar in appearance to catalysts in other batches, exhibiting small 2–5 nm particles on the TEM and rounded larger particles on the SEM. This difference is illustrated in Figure 3.

Although there was no apparent difference in the large particles for catalysts of batch C, for the catalysts dried in the rotary evaporator (C60, C80, and C100) the smaller particles observed on the TEM are visible on the SEM, whereas for all other catalysts they were not visible. They appear also to be uniformly dispersed across the catalyst surface (see Figure 4). The sizes of the crystallites cannot be measured by SEM as at that level of magnification particles of that size cannot be properly resolved. The only difference in the preparation of these catalysts is that they were dried in a rotary evaporator at reduced pressure rather than in an oven or in flowing air. It has been shown that for cases were the metal is weakly adsorbed the method of drying can strongly impact the final distribution of the metal on the support[15,16].

Oxygen chemisorption

Catalysts were further characterized using high-temperature oxygen chemisorption. An example of the oxygen take-up as a function of the oxygen pressure is given in Figure 5. All catalysts display the same characteristic curve shape, with the volume adsorbed varying slightly from catalyst to catalyst, with an uptake at low pressure reaching saturation at an oxygen partial pressure of 2 mm Hg, and then increasing further in the range beyond 5 mm Hg. This is indicative of a dual site adsorption mechanism with a strong adsorbing site (saturated with O_2 at low pressure) and a weakly adsorbing site. The latter may be the support, which is known to adsorb oxygen[17].

Characterization of Au catalysts

Table III

Average particle sizes obtained from electron microscopy (in nm)

Catalyst	TEM size [no. of particles]	SEM size [no. of particles]
A1-200	2.25 ± 0.73 [20]	171 ± 77 [120]
A1-500	2.68 ± 0.91 [69]	134 ± 72 [82]
A2-200Ar	2.65 ± 0.81 [54]	220 ± 89 [7]
A2-500Ar	3.17 ± 1.08 [45]	
A2-200H	2.07 ± 0.65 [68]	93 ± 80 [99]
A2-500H	3.17 ± 0.91 [71]	230 [1]
B-base	4.11 ± 1.41 [146]	146 ± 38 [5]
B-time	5.18 ± 1.57 [40]	210 ± 172 [24]
B-ratio		129 ± 51 [8]
B-conc	4.33 ± 1.86 [113]	73 ± 66 [10]
B-none	N/A	N/A
C-DRY	2.87 ± 0.87 [79]	100 ± 93 [56]
C-WET	2.66 ± 0.65 [101]	377 ± 62 [2]
C60	3.00 ± 1.05 [66]	98 ± 101 [15]
C80	2.21 ± 0.48 [103]	147 ± 124 [5]
C100	2.59 ± 0.79 [105]	82 ± 43 [25]
D100	4.16 ± 1.43 [102]	240 ± 130nm [52]
D200	4.41 ± 1.81 [103]	150 ± 80nm [86]
D300	3.04 ± 1.13 [154]	110 ± 90 [86]
D400	2.88 ± 1.01 [85]	180 ± 170 [45]
D500	3.09 ± 0.99 [102]	100 ± 30 [83]

Conclusions

The SEM and TEM images of the catalysts clearly show that certain preparation variables affect the formation and presence of large (>50 nm) gold crystallites as well as the dispersion of the small (2–5 nm) gold crystallites on alumina-supported gold catalysts. The concentration of the precursor solution and the conditions of calcination within the parameters investigated have no significant effect on the presence of large gold crystallites or the particle size distribution of the small crystallites.

The ammonia washing step plays an important role in the formation of large gold crystallites. A shorter, more dilute, or smaller volume wash does not prevent the usual formation of small 2–5 nm gold crystallites. However, complete omission of this step results in a catalyst containing only gold particles upwards of 50 nm in size.

The drying step plays an important role in the dispersion of the small gold crystallites while not affecting the presence of the larger ones. Catalysts dried in the rotary evaporator display well-dispersed crystallites that are visible on the SEM. Further characterization and catalyst testing will determine whether this affects the overall performance of the catalyst.

Acknowledgements

Mrs. H. Divey, Mrs. S. Vasic, and Mr L. Mtebeni, for assistance with digestions, AAS, chemisorption and TPD in

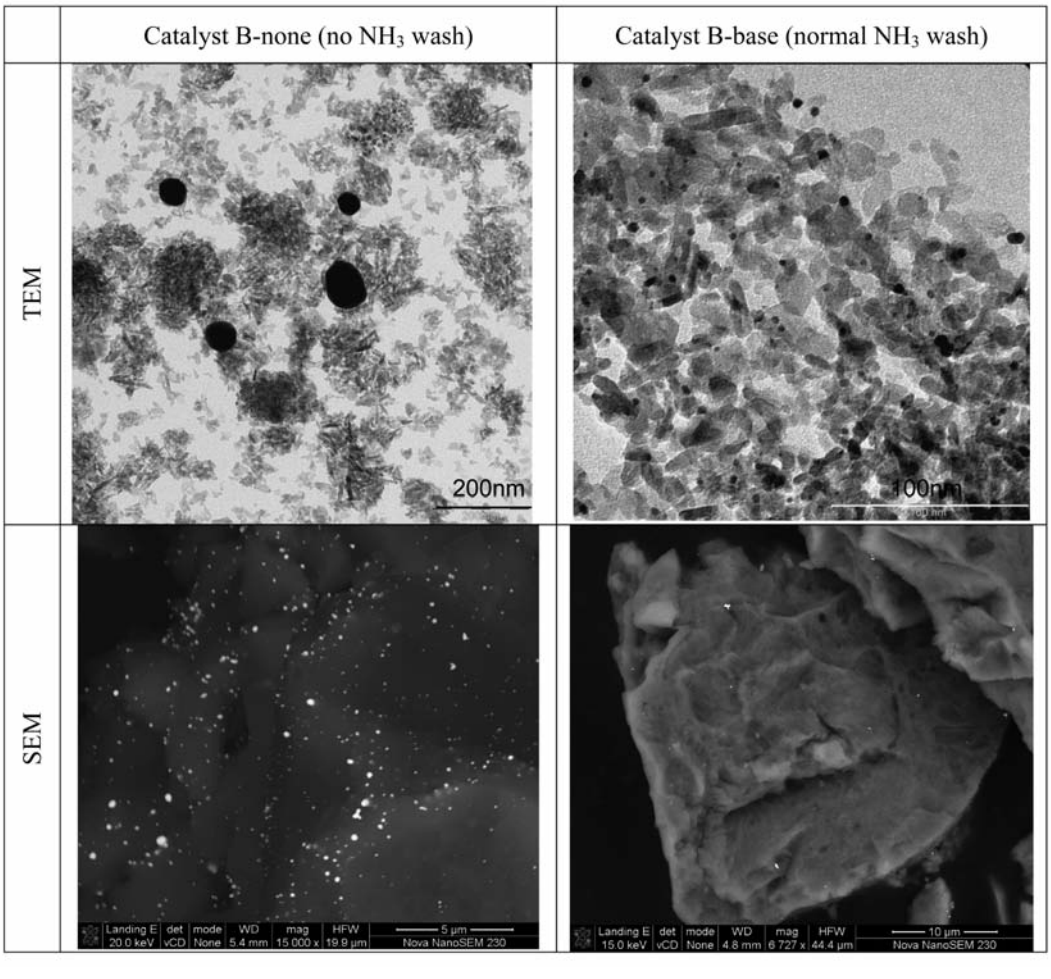

Figure 3—Examples of TEM and SEM images illustrating the effect of the ammonia washing step in batch B

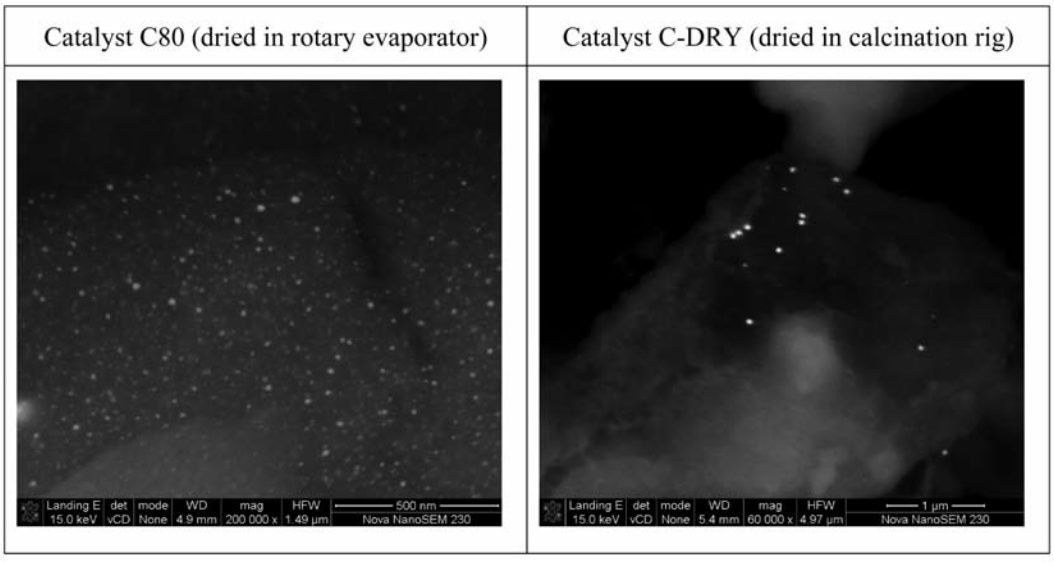

Figure 4—Examples of SEM-images for Batch C showing a difference in small crystallite dispersion with changes in drying conditions

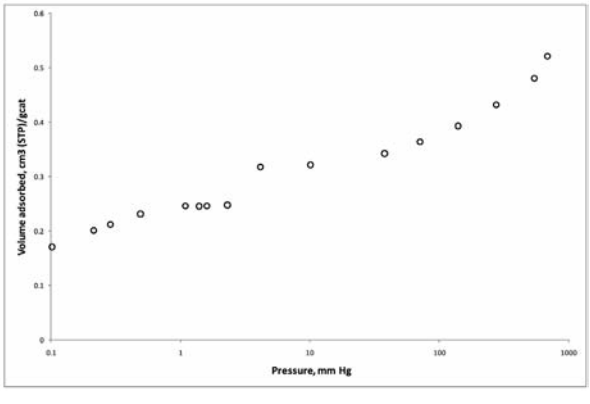

Figure 5—Oxygen take-up at 200°C for catalyst D300

the analytical laboratory. Mr M. Jaffer, Ms M. Waldron, and Mr F. Cummings, for assistance with the various electron microscopes. Financial assistance from Mintek, the NRF, and UCT is also gratefully acknowledged.

References

1. Haruta, M. Size- and support-dependency in the catalysis of gold. *Catalysis Today*, vol. 36, no. 1, 1997. pp. 153–166.
2. Sakurai, H., and Haruta, M. Carbon dioxide and carbon monoxide hydrogenation over gold supported on titanium, iron, and zinc oxides. *Applied Catalysis A*: General, vol. 127, nos. 1–2, 1995. pp. 93–105.
3. Sakurai, H., and Haruta, M. Synergism in methanol synthesis from carbon dioxide over gold catalysts supported on metal oxides. *Catalysis Today*, vol. 29, nos. 1–4, 1996. pp. 361–365.
4. Zhao, Y., Mpela, A., Enache, D.I., Taylor, S.H., Hildebrandt, D., Glasser, D., Hutchings, G. J., Atkins, M.P., and Scurrel, M.S. Study of carbon monoxide hydrogenation over supported Au catalysts. *Studies in Surface Science and Catalysis*, vol. 163, (Fischer-Tropsch synthesis, catalysts and catalysis), 2007. pp. 141–151.
5. Haruta, M, Tsubota, S., Kobayashi, T., Kageyama, H., Genet, M.J., and Delmon, B. Low-temperature oxidation of CO over gold supported on TiO_2, α-Fe_2O_3, and Co_3O_4. *Journal of Catalysis*, vol. 144, no. 1, 1993. pp. 175–192.
6. Baatz, C., Decker, N., and Pruse, U. New innovative gold catalysts prepared by an improved incipient wetness method. *Journal of Catalysis*, vol. 258, no. 1, 2008. pp. 165–169.
7. Barkuizen, D., Mabaso, I., Viljoen, E., Welker, C., Claeys, M., van Steen, E., and Fletcher, J.C.Q. Experimental approaches to the preparation of supported metal nanoparticles. *Advanced Materials*, vol. 78, no. 9, 2006. pp. 1759–1769.
8. Hugon, A., Kollie, N.E., and Louis, C. Advances in the preparation of supported gold catalysts: Mechanism of deposition, simplification of the procedures and relevance of the elimination of chlorine. *Journal of Catalysis*, vol. 274, no. 2, 2010. pp. 239–250.
9. Ivanova, S., Petit, C., and Pitchon, V. A new preparation method for the formation of gold nanoparticles on an oxide support. *Applied Catalysis A: General*, vol. 267, 2004. pp. 191–201.
10. Xu, Q., Meng, G., Chen, B., Li, X., Zhu, X., Chu, Z., and Kong, M. Synthesis of AuNi/NiO nanocables by Porous AAO template assisted galvanic deposition and subsequent oxidation. *European Journal of Inorganic Chemistry*, vol. 2010, no. 27, 2010. pp. 4309–4313.
11. Ivanova, S., Pitchon, V., Zimmermann, Y., and Petit, C. Preparation of alumina supported gold catalysts: Influence of washing procedures, mechanism of particles size growth. *Applied Catalysis A: General*, vol. 298, 2006. pp. 57–64.
12. Oh, H.-S., Yang, J.H., Costello, C.K., Wang, Y.M., Bare, S.R., Kung, H.H., and Kung, M.C. Selective catalytic oxidation of CO: effect of chloride on supported Au catalysts. *Journal of Catalysis*, vol. 210, 2002. pp. 375–386.
13. Yang, J., Henao, J., Costello, C., Kung, M., Kung, H., Miller, J., Kropf, A., Kim, J., Regalbuto, J., and Bore, M. Understanding preparation variables in the synthesis of Au/AlO using EXAFS and electron microscopy. *Applied Catalysis A: General*, vol. 291, no's. 1–2, 2005. pp. 73–84.
14. Berndt, H., Pitsch, I., Evert, S., Struve, K., Pohl, M., Radnik, J., and Martin, A. Oxygen adsorption on Au/Al_2O_3 catalysts and relation to the catalytic oxidation of ethylene glycol to glycolic acid. *Applied Catalysis*, vol. 244, 2003. pp. 169–179.
15. Lekhal, A., Glasser, B.J., and Khinast, J.G. Impact of drying on the catalyst profile in supported impregnation catalysts. *Chemical Engineering Science*, vol. 56, no. 15, 2001. pp. 4473–4487.
16. Santhanam, N., Conforti, T.A., and Spieker, W. Nature of metal catalyst precursors adsorbed onto oxide supports. *Catalysis Today*, vol. 21, 1994. pp. 141–156.
17. Xu, Q, Kharas, K.C.C., and Datye, A.K. The preparation of highly dispersed Au/Al_2O_3 by aqueous impregnation. *Catalysis Letters*, vol. 85, 2003. pp. 229–235. ◆